Quark Matter in Neutron Stars

William M. Spinella, Fridolin Weber, Gustavo A. Contrera and Milva G. Orsaria

Abstract The nonlocal three-flavor Nambu-Jona-Lasinio model is used to study quark deconfinement in the cores of neutron stars (NSs). The quark-hadron phase transition is modeled using both the Maxwell construction and the Gibbs construction. For the Maxwell construction, we find that all NSs with core densities beyond the phase transition density are unstable. Therefore, no quark matter cores would exist inside such NSs. The situation is drastically different if the phase transition is treated as a Gibbs transition, resulting in stable NSs whose stellar cores are a mixture of hadronic matter and deconfined quarks. The largest fractions of quarks achieved in the quark-hadron mixed phase are around 50%. No choice of parametrization or composition leads to a pure quark matter core. The inclusion of repulsive vector interactions among the quarks is crucial since the equation of state (EoS) in the quark-hadron mixed phase is significantly softer than that of the pure hadronic phase.

W. M. Spinella (✉)
School of Physical Sciences and Technologies, Irvine Valley College, 5550 Irvine Center Drive, Irvine, CA 92618, USA
e-mail: wspinella@ivc.edu

F. Weber
Department of Physics, San Diego State University, 5500 Campanile Drive, San Diego, CA 92182, USA
e-mail: fweber@sdsu.edu

Center for Astrophysics and Space Sciences, University of California, San Diego, La Jolla, CA 92093, USA

G. A. Contrera
Facultad de Ciencias Exactas, IFLP, UNLP, CONICET, Diagonal 113 entre 63 y 64, La Plata 1900, Argentina
e-mail: contrera@fisica.unlp.edu.ar

G. A. Contrera · M. G. Orsaria
Grupo de Gravitación, Astrofísica y Cosmología,
Facultad de Ciencias Astronómicas y Geofísicas, Universidad Nacional de La Plata, Paseo del Bosque S/N (1900), La Plata, Argentina
e-mail: morsaria@fcaglp.unlp.edu.ar

CONICET, Godoy Cruz 2290, C1425FQB Buenos Aires, Argentina

J. Kirsch et al. (eds.), *Discoveries at the Frontiers of Science*,
FIAS Interdisciplinary Science Series, https://doi.org/10.1007/978-3-030-34234-0_9

1 Introduction

Neutron stars (NSs) are among the most dense astrophysical objects in the Universe [1]. They have radii of around 12km and masses up to an observed $2.01\,M_\odot$ [2–4]. This suggests that these objects have extreme central densities on the order of $10^{15}\,\mathrm{g/cm^3}$, greater than the density of an atomic nucleus which is about $2.5 \times 10^{14}\,\mathrm{g/cm^3}$. At such extreme densities the primary constituents of NS matter are neutrons, protons, electrons and muons, and possibly also hyperons [5, 6], the delta isobar $\Delta(1232)$ [7], and/or deconfined quarks [8, 9]. More than that, if deconfined quarks should exist in the cores of neutron stars, they are likely to be in a color superconducting state (see, for instance, [10–12] and references therein). Investigating the possible existence of these building blocks of matter in the cores of neutron stars is a very active area of research [13] and the focus of this short review paper. A detailed discussion of the material presented here can be found in [14].

2 Description of Quark Matter

In this paper quark matter is described by an improved version of the nonlocal SU(3) Nambu-Jona-Lasinio (n3NJL) model [15, 16], which treats the quark-quark interaction as a one-gluon exchange [17, 18]. A unique scalar (σ_f) and vector (ω_f) field is assigned to each quark flavor and an additional mixing interaction is included. These interactions are parametrized by the coupling constants of the model: G_S is the strong coupling constant, G_V is the vector coupling constant, and H is the coupling constant associated with mixing. The quark masses $m_u = m_d$ and m_s, G_S, H, and the nonlocality parameter $\Lambda_{\rm nl}$ are determined by fitting the model to empirical values of the pion mass and decay constant (m_π, f_π), and the pseudoscalar η' meson mass ($m_{\eta'}$), while the vacuum pressure (Ω_0) is determined by imposing that the nonlocal thermodynamic potential equal zero at zero temperature and chemical potential, i.e., $\Omega_0 - \Omega^{\rm NL}(M, T = 0, \mu = 0) = 0$ [17–19]. The n3NJL parametrizations are provided in Table 1. In the mean-field approximation the thermodynamic potential of the model is given by [15, 16]

Table 1 Parametrizations of the n3NJL model [20]

Parameters	P119	P127
$m_u = m_d$ (MeV)	5.0	5.5
m_s (MeV)	119.3	127.8
$\Lambda_{\rm nl}$ (MeV)	843.0	780.6
$G_S\Lambda_{\rm nl}^2$ (MeV^2)	13.34	14.48
$H\Lambda_{\rm nl}^5$ (MeV^5)	−273.75	−267.24
Ω_0 (MeV/fm^3)	−239.51	−243.85

$$\Omega^{\rm NL}(M,T=0,\mu) = -\frac{3}{\pi^3}\sum_f \int_0^\infty dk_0 \int_0^\infty dk\, \ln\left[\left[\widehat{p}_f^2 + M_f^2(p_f)\right]\frac{1}{p_f^2+m_f^2}\right]$$
$$-\frac{3}{\pi^2}\sum_f \int_0^{\sqrt{\mu_f^2-m_f^2}} dk\, k^2\left[\left(\mu_f - E_f\right)\theta\left(\mu_f - m_f\right)\right]$$
$$-\frac{1}{2}\Bigg[\sum_f\left(\bar{\sigma}_f\bar{S}_f + \frac{G_S}{2}\bar{S}_f^2\right) + \frac{H}{2}\bar{S}_u\,\bar{S}_d\,\bar{S}_s\Bigg] - \sum_f \frac{\bar{\omega}_f^2}{4G_V}\,, \tag{1}$$

where $f \in \{u,d,s\}$ is the quark flavor, $\bar{\sigma}_f$ and $\bar{\omega}_f$, are the quark scalar and vector mean fields respectively, $E_f = \sqrt{k^2+m_f^2}$ is the quark energy, $p_f^2 = (k_0 + i\mu_f)^2 + k^2$ is the quark four momentum, and $\bar{S}_f$ is the quark auxiliary field given by [15, 16]

$$\bar{S}_f = -\frac{6}{\pi^3}\int_0^\infty dk_0 \int_0^\infty dk\, g(p_f)\,\frac{M_f(p_f)}{\widehat{p}^2 + M_f^2(p_f)}\,. \tag{2}$$

The dynamical quark mass $M_f(p_f) = m_f + \bar{\sigma}_f g(p_f)$ depends on the form factor $g(p_f) = \exp(-p_f^2/\Lambda_{\rm nl}^2)$, which makes the model more consistent with results from lattice QCD calculations [21]. The scalar and vector mean field equations can be found by minimizing $\Omega^{\rm NL}$ with respect to the fields,

$$\frac{\partial\Omega^{\rm NL}}{\partial\bar{\sigma}_f} = \bar{\sigma}_f + G_S\bar{S}_f + \frac{1}{2}H\bar{S}_i\bar{S}_j = 0\,, \quad \frac{\partial\Omega^{\rm NL}}{\partial\bar{\omega}_f} = \bar{\omega}_f - 2G_V\frac{\partial\Omega^{\rm NL}}{\partial p_f} = 0\,, \tag{3}$$

for $f \in \{u,d,s\}$ and $i \neq j \neq f$. The simultaneous solution of this system is subject to the conditions of charge neutrality and baryon number conservation,

$$\sum_f n_f q_f + \sum_\lambda n_\lambda q_\lambda = 0\,, \quad n - \frac{1}{3}\sum_f n_f = 0\,, \tag{4}$$

respectively, determines the mean fields ($\bar{\sigma}_f, \bar{\omega}_f$, $f \in \{u,d,s\}$) and the baryon and electron chemical potentials (μ_n, μ_e). The individual quark chemical potentials are then specified by the chemical equilibrium condition

$$\mu_f = \frac{1}{3}\left(\mu_n - 3\,q_f\,\mu_e\right) \tag{5}$$

and the particle number densities follow from $n_f = \partial\Omega^{\rm NL}/\partial\mu_f$. The total pressure of the system comes from the quarks, leptons, and the vacuum and is given by

$$P_{\rm n3NJL} = \Omega_0 - \Omega^{\rm NL} - \Omega_l\,, \tag{6}$$

where Ω_0 is fixed by the condition that Eq. 1 vanishes at $T = \mu_f = 0$, and Ω_1 denotes the lepton thermodynamic potential given by

$$\Omega_l = -\frac{1}{12\pi^2}\sum_\lambda \left[\mu_\lambda\sqrt{\mu_\lambda^2 - m_\lambda^2}\left(\mu_\lambda^2 - \frac{5}{2}m_\lambda^2\right) + \frac{3}{2}m_\lambda^4 \ln\left(\frac{\mu_\lambda + \sqrt{\mu_\lambda^2 + m_\lambda^2}}{m_\lambda}\right)\right]. \quad (7)$$

Finally, the total energy density of the system is given by

$$\mathscr{E}_{\text{n3NJL}} = -P_{\text{n3NJL}} + \sum_f n_f\ \mu_f + \sum_\lambda n_\lambda\ \mu_\lambda. \quad (8)$$

3 EoS of Quark-Hybrid Matter and Neutron Star Structure

Allowing for the possibility of quark deconfinement, a quark-hadron phase transition may commence when the pressure of the quark phase equals that of the hadronic phase. The nature of the phase transition depends on the surface tension, α, between the two phases that is still quite uncertain. Recent works have typically placed $\alpha \lesssim 30$ MeV/fm^2, though there are suggestions that values greater than 100 MeV/fm^2 could be possible too [22–25]. If $\alpha \gtrsim 70$ MeV/fm^2 the quark-hadron phase transition will be one of constant pressure with an equation of state that is discontinuous in energy density [26, 27]. The result is a sharp interface between phases of pure hadronic matter and pure quark matter at a given NS radius, as shown schematically in Fig. 1.

The phase transition is achieved by applying the Maxwell construction (at zero temperature, T)

$$P_H(\mu_n, T = 0) = P_Q(\mu_n, T = 0), \quad (9)$$

where μ_n is the neutron chemical potential, and P_H and P_Q represent the pressure of the hadronic and the quark phase, respectively. Alternatively, if $\alpha \lesssim 70$ MeV/fm^2 the phase transition results in the formation of a stable coexistent (mixed) phase, gradually converting NS matter from hadronic matter to deconfined quark matter with increasing density, as shown in Fig. 2. This phase transition satisfies the Gibbs

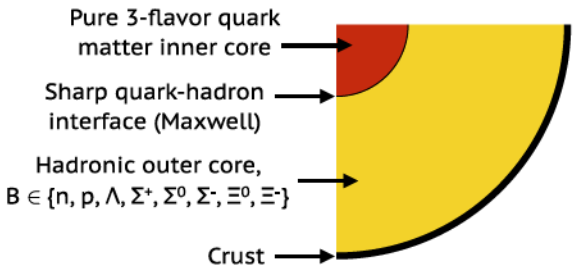

Fig. 1 Hypothetical NS cross section assuming a constant pressure (Maxwell construction) phase transition from hadronic matter to a pure quark matter core [14]

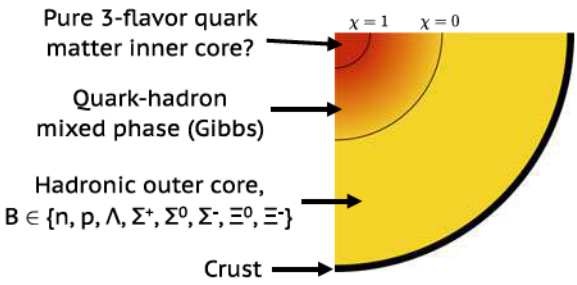

Fig. 2 Hypothetical NS cross section assuming a phase transition from hadronic matter to a quark-hadron mixed phase (Gibbs construction) and possibly a pure quark matter core [14]

condition for phase equilibrium,

$$P_H\left(\mu_n, \mu_e, T=0\right) = P_Q\left(\mu_n, \mu_e, T=0\right), \tag{10}$$

where μ_e is the electron chemical potential. The isospin restoring force favors a positively charged hadronic phase as an increased number of protons reduces isospin asymmetry. This necessarily results in a negatively charged quark phase, electric charge neutrality being achieved globally. Competition between the Coulomb and surface energies will cause the phases to arrange themselves into energy minimizing geometric configurations [28]. This rearrangement and its effect on neutrino emissivity were investigated in [29, 30].

A popular model used to determine P_H is the relativistic mean-field (RMF) theory [31, 32], which is based on a lagrangian of the following type [33–36],

$$\begin{aligned}\mathscr{L} = &\sum_B \bar{\psi}_B\left[\gamma_\mu(i\partial^\mu - g_\omega\omega^\mu - \frac{1}{2}g_\rho\boldsymbol{\tau}\cdot\boldsymbol{\rho}^\mu) - (m_N - g_\sigma\sigma)\right]\psi_B \\ &+ \frac{1}{2}(\partial_\mu\sigma\partial^\mu\sigma - m_\sigma^2\sigma^2) - \frac{1}{3}b_\sigma m_N(g_\sigma\sigma)^3 - \frac{1}{4}c_\sigma(g_\sigma\sigma)^4 - \frac{1}{4}\omega_{\mu\nu}\,\omega^{\mu\nu} \\ &+ \frac{1}{2}m_\omega^2\,\omega_\mu\,\omega^\mu + \frac{1}{2}m_\rho^2\,\boldsymbol{\rho}_\mu\cdot\boldsymbol{\rho}^\mu - \frac{1}{4}\boldsymbol{\rho}_{\mu\nu}\,\boldsymbol{\rho}^{\mu\nu} + \sum_{\lambda=e^-,\mu^-}\bar{\psi}_\lambda(i\gamma_\mu\partial^\mu - m_\lambda)\psi_\lambda\,.\end{aligned} \tag{11}$$

This lagrangian describes baryons interacting via the exchange of scalar, vector, and isovector mesons (σ, ω, $\boldsymbol{\rho}$, respectively). The sum over B sums all baryon states that are present in neutron star matter at a given density. The quantities g_ρ, g_σ, and g_ω are the meson-baryon coupling constants. The coupling constants of cubic and quartic σ-meson self-interactions are denoted b_σ and c_σ. The quantities $\omega^{\mu\nu}$ ($= \partial^\mu\omega^\nu - \partial^\nu\omega^\mu$) and $\boldsymbol{\rho}^{\mu\nu}$ ($= \partial^\mu\boldsymbol{\rho}^\nu - \partial^\nu\boldsymbol{\rho}^\mu$) denote meson field tensors. The RMF approach is parametrized to reproduce the properties of symmetric nuclear matter at saturation density n_0 (see Table 2): the binding energy per nucleon (E_0), the nuclear incompressibility (K_0), the isospin asymmetry energy (J), and the effective mass (m^*/m_N). In addition, the RMF parametrizations used in this work employ a density-dependent isovector-meson-baryon coupling constant that can be fit to the slope of the asymmetry energy (L_0) at n_0, and the DD2 and ME2 parametrizations scalar-

Table 2 Properties of nuclear matter at saturation density for the hadronic parametrizations of this work

Saturation property	SWL [14]	GM1L [14, 37]	DD2 [38]	ME2 [39]
n_0 (fm^{-3})	0.150	0.153	0.149	0.152
E_0 (MeV)	−16.00	−16.30	−16.02	−16.14
K_0 (MeV)	260.0	300.0	242.7	250.9
m^*/m_N	0.70	0.70	0.56	0.57
J (MeV)	31.0	32.5	32.8	32.3
L_0 (MeV)	55.0	55.0	55.3	51.3

and vector-meson-baryon coupling constants are also density-dependent and are fit to properties of finite nuclei [14, 38, 39].

For the Gibbs transition (10), the nonlinear systems of equations following from (3) and (11) must be solved simultaneously along with the global charge neutrality condition

$$\sum_B n_B q_B + \sum_f n_f q_f + \sum_\lambda n_\lambda q_\lambda = 0\,, \tag{12}$$

where n_B denotes the number density of baryon B carrying an electric charge q_B. To parametrize the amount of quark matter in the mixed phase, the parameter χ is introduced, which represents the volume fraction of quark matter at a given density. This parameter enters into the nonlinear, coupled system of equations through the condition of baryon number conservation,

$$n - (1-\chi)\sum_B n_B - \frac{1}{3}\chi\sum_f n_f = 0\,. \tag{13}$$

The EoS can then be calculated from the relations

$$\varepsilon_{HQ} = (1-\chi)\varepsilon_H + \chi\varepsilon_Q\,, \quad P_{HQ} = \frac{1}{2}\left(P_H + P_Q\right)\,, \tag{14}$$

where ε_H and ε_Q are the respective energy densities of hadronic matter and quark matter in the mixed phase.

The system of Eqs. (3) and (11) is easier to solve for the Maxwell phase transition (9), where hadronic matter and quark matter are separately charge neutral and in chemical equilibrium so that Eqs. (3) and (11) are decoupled.

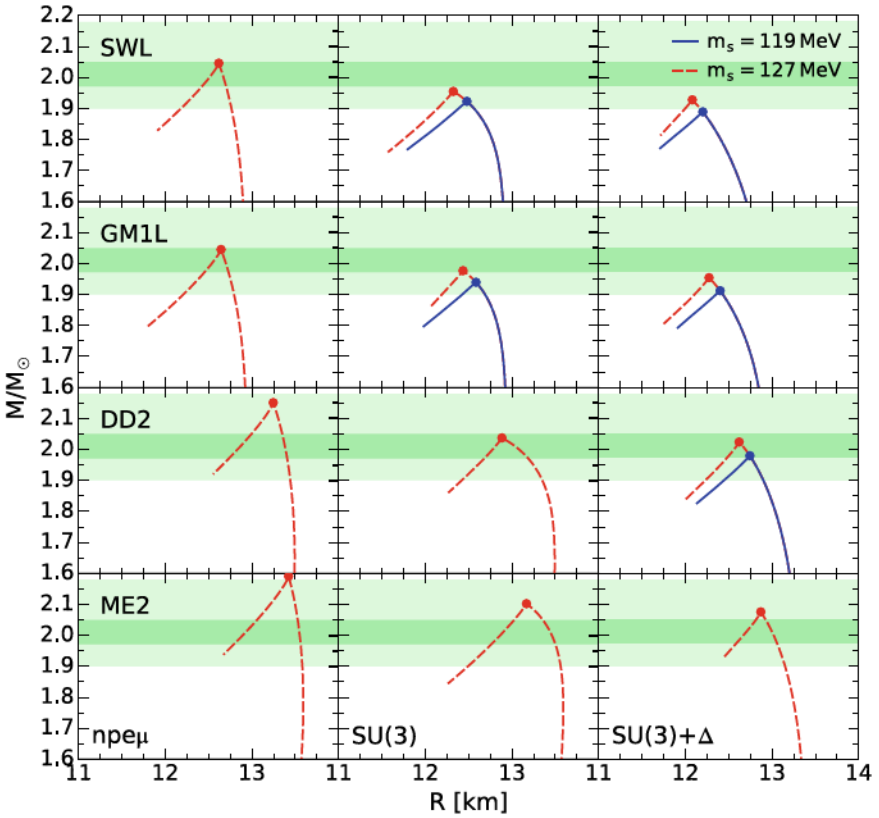

Fig. 3 Mass versus radius for NSs with a phase transition from hadronic matter to deconfined quark matter modeled using the Maxwell construction [14]. The dark (light) green shading indicates the 1σ (3σ) uncertainty range in the mass of PSR J0348+0432. The circle markers indicate the location of the phase transition which happens to coincide with the maximum mass for all parametrizations and compositions. (Left column) Only nucleons and leptons are included in the hadronic phase. (Center column) Hyperons are included with the vector meson-hyperon coupling constants given by the SU(3) ESC08 model. (Right column) Delta isobars are also included with the following couplings: $x_{\sigma\Delta} = x_{\omega\Delta} = 1.1$ and $x_{\rho\Delta} = 1.0$

3.1 The Maxwell Phase Transition

The mass-radius curves for quark-hadron hybrid EoSs constructed for the Maxwell transition with the P119 and P127 n3NJL parametrization are given in Fig. 3. EoSs that include pure deconfined quark matter are too soft to support stable NSs for all particle configurations and parametrizations. One interesting interpretation of this result is that the phase transition to deconfined quark matter is the limiting factor for the NS mass and density. Further, almost all configurations in Fig. 3 are consistent with the mass constraint set by PSR J0348+0432 at the 1σ level, with the exception of

SWL with hyperons and Δs, and GM1L with Δs, both satisfying the mass constraint only at 3σ. Finally, no vector coupling was considered in the n3NJL EoS as this would simply lead to even higher density phase transitions guaranteed to result in the same instability as observed for $G_V = 0$.

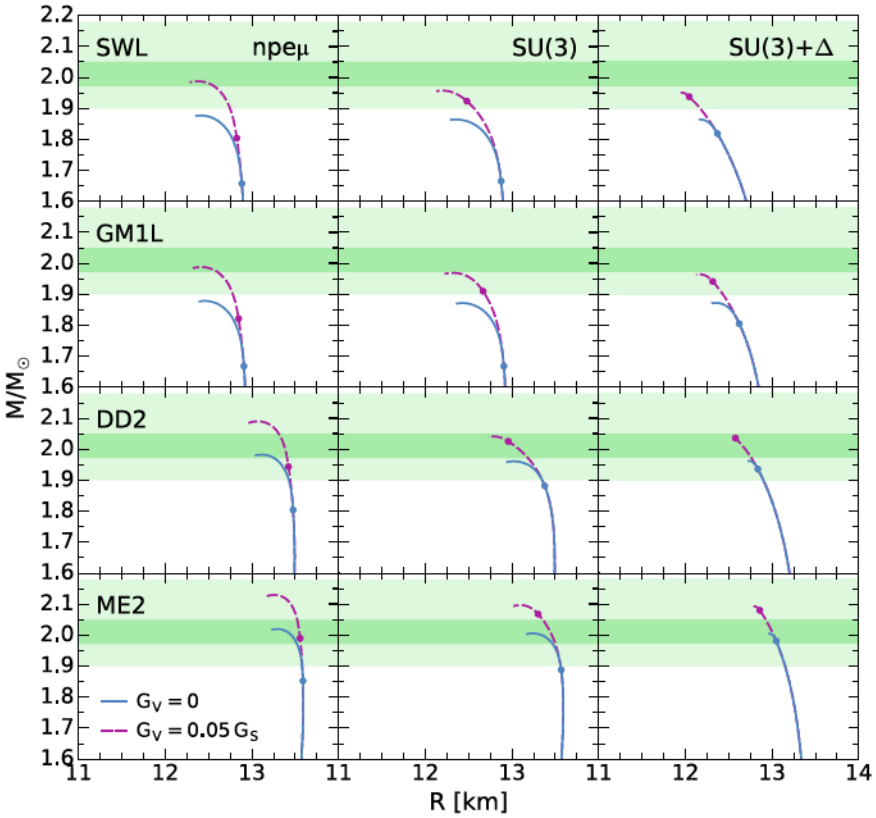

Fig. 4 The mass versus radius for NSs with a phase transition from hadronic matter to deconfined quark matter modeled using the Gibbs construction and the P119 n3NJL parametrization [14]. The dark (light) green shading indicates the 1σ (3σ) uncertainty range in the mass of PSR J0348+0432. The circle markers indicate the location of the phase transition. (Left column) Only nucleons and leptons are included in the hadronic phase. (Center column) Hyperons are included with the vector meson-hyperon coupling constants given by the SU(3) ESC08 model. (Right column) Delta isobars are also included with the following couplings: $x_{\sigma\Delta} = x_{\omega\Delta} = 1.1$ and $x_{\rho\Delta} = 1.0$

3.2 The Gibbs Phase Transition

The mass-radius curves for quark-hadron hybrid EoSs constructed using the Gibbs transition with the P119 n3NJL parametrization are given in Fig. 4. As an extreme we can first consider a quark-hadron hybrid EoS in the absence of hyperons or Δs ($npe\mu$ matter). In this case the SWL and GM1L parametrizations require the inclusion of the vector interaction to be consistent with the mass constraint, the maximum falling in the 1σ range. The DD2 and ME2 parametrizations satisfy the mass constraint at the 1σ level without requiring the inclusion of the vector interaction. All parametrizations have a fairly discoverable 0.15–0.2 $M_\odot$ range in the mass-radius curve in which a quark-hadron mixed phase appears in the core. The phase transition occurs in the fairly low density range 2.5–3 n_0, leading to quark matter fractions of 38–45% in the core. Free quarks are found to make up as much 4–6.3% of the total quarks in a NS, accounting for 6–8.8% of the total mass, both fractions increasing with the softness of the EoS.

Hyperons are included in all parametrizations with the vector meson-hyperon coupling constants given by the SU(3) ESC08 model [40]. The presence of hyperons lowers the maximum mass by less than 2% in almost all cases (exception DD2 with vector interaction), and moves the SWL and GM1L parametrizations outside the 1σ range of the mass constraint even with the inclusion of the vector interaction. The DD2 parametrization with hyperons requires the vector interaction to satisfy the mass constraint, while ME2 still does not. Without the vector interaction the quark-hadron mixed phase exists in about a 0.2 $M_\odot$ range for SWL and GM1L, but a smaller somewhat less discoverable $0.08 - 0.12\,M_\odot$ range for DD2 and ME2. Including the vector interaction reduces the overall mixed phase mass range to $\lesssim 0.06\,M_\odot$, with a range of only 0.01 $M_\odot$ for DD2, seriously limiting discoverability. Hyperons soften the EoS delaying the quark-hadron phase transition slightly without the vector interaction but drastically when the vector interaction is included. The quark matter fraction in the core reaches 35–42%, smaller than with the purely nucleonic hadronic EoSs, with a similar decrease in the total quark matter fraction and quark matter mass fraction.

Including Δs in addition to hyperons further delays the onset of the quark-hadron phase transition. However, the quark-hadron mixed phase EoS with Δs is very soft, with the result that the maximum masses are almost the same as with hyperons alone. The critical masses are within 0.02 $M_\odot$ of the maximum mass (excluding SWL for $G_V = 0$), leaving an extremely small range for discoverability. Surprisingly, in this small mass range the highest mixed phase quark matter fractions are achieved at almost 50%. However, even with these large χ values the high critical density indicates an extended hadronic phase and leads to a total quark matter fraction and quark matter mass fraction that are comparatively small.

Figure 5 shows the particle number densities for the DD2 parametrization for all particle configurations both with and without the vector interaction. Charge neutrality and the reduction of isospin asymmetry drive the NS composition in the quark-hadron mixed phase. At the onset the negatively charged d quark dominates the other quarks

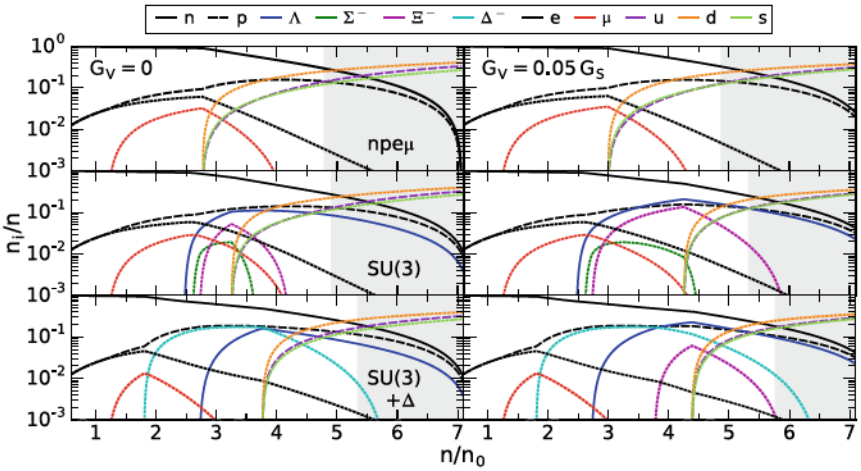

Fig. 5 The relative number density of particles as a function of baryon number density (in units of the saturation density) for the DD2 parametrization [14]. The gray shading indicates baryon number densities beyond the maximum. (Top row) Only nucleons and leptons are included in the hadronic phase. (Center row) Hyperons are included with the vector meson-hyperon coupling constants given by the SU(3) ESC08 model. (Bottom row) Delta isobars are also included with the following couplings: $x_{\sigma\Delta} = x_{\omega\Delta} = 1.1$ and $x_{\rho\Delta} = 1.0$

and replaces high energy leptons and negatively charged baryons. The s quark has a relatively high mass for a quark but it is still quite low compared to the baryons, so it also helps remove high energy leptons and negatively charged baryons from the system. The positively charged u quark replaces high energy protons and has a positive isospin ($I_u = +1/2$) which helps reduce isospin asymmetry. In $npe\mu$ and hyperonic matter the proton number density actually continues to increase at the onset of the mixed phase reducing isospin asymmetry. The negatively charged hyperons and Δs on the other hand all rapidly decline in number density, vanishing before the end of the mixed phase. Finally, the protons, neutrons, and Λs all exist up to the limit of the mixed phase.

4 Summary

We presented the nonlocal SU(3) Nambu-Jona-Lasinio model for the modeling of deconfined quark matter, and combined it with different quantum hadrodynamical models (RMFL, DDRMF) [14] to construct models for the quark-hadron hybrid EoS. The quark-hadron phase transition was modeled using the Maxwell construction given a high surface tension ($\gtrsim 70\,\mathrm{MeV/fm^2}$), and it was found that NSs with core densities beyond the phase transition density are unstable. Therefore, no pure quark matter core exists and the phase transition mass marks the endpoint of the NS mass-

radius curve. Given a relatively low surface tension ($\lesssim 70\,\mathrm{MeV/fm^2}$) the quark-hadron phase transition was modeled using the Gibbs construction, resulting in a stable NS core where hadronic and deconfined quark matter coexist. The largest fractions of quark matter achieved in the quark-hadron mixed phase were around 50%; no choice of parametrization or composition led to a pure quark matter core. Finally, hybrid EoSs employing the SWL and GM1L hadronic parametrizations were shown to require the vector interaction to satisfy the mass constraint set by PSR J0348+0432.

Acknowledgements G.A.C. and M.G.O. thank CONICET and UNLP for financial support under Grants PIP 0714, G 140, G157, and X824. F.W. is supported by the National Science Foundation (USA) under Grants PHY-1411708 and PHY-1714068.

References

1. W. Becker (ed.), *Neutron Stars and Pulsars, Astrophysics and Space Science Library*, vol. 357 (Springer, 2009)
2. J. Antoniadis et al., Science **340**, 6131 (2013)
3. P. Demorest, T. Pennucci, S. Ransom, M. Roberts, J. Hessels, Nature **467**, 1018 (2010)
4. E. Fonseca et al., Astrophys. J. **832**, 167 (2016)
5. V.A. Ambartsumyan, G.S. Saakyan, Sov. Ast. **4**, 187 (1960)
6. N.K. Glendenning, Astrophys. J. **293**, 470 (1985)
7. A. Drago, A. Lavagno, G. Pagliara, Phys. Rev. D **89**, 043014 (2014); A. Drago, A. Lavagno, G. Pagliara, Daniele Pigato, Phys. Rev. D **90**, 065809 (2014)
8. D.D. Ivanenko, D.F. Kurdgelaidze, Astrophysics **1**, 251 (1965)
9. H. Fritzsch, M. Gell-Mann, H. Leutwyler, Phys. Lett. **47B**, 365 (1973)
10. K. Rajagopal, F. Wilczek, The condensed matter physics of QCD, in *At the Frontier of Particle Physics* (World Scientific, 2001), pp. 2061–2151
11. M.G. Alford, K. Rajagopal, T. Schaefer, A. Schmitt, Rev. Mod. Phys. **80**, 1455 (2008)
12. I.F. Ranea-Sandoval, M.G. Orsaria, S. Han, F. Weber, W.M. Spinella, Phys. Rev. D **96**, 065807 (2018)
13. M. Buballa et al., J. Phys. G: Nucl. Part. Phys. **41**, 123001 (2014)
14. W.M. Spinella, A Systematic Investigation of Exotic Matter in Neutron Stars. Ph.D. thesis, Claremont Graduate University & San Diego State University (2017)
15. M. Orsaria, H. Rodrigues, F. Weber, G.A. Contrera, Phys. Rev. C **87**, 023001 (2013)
16. M. Orsaria, H. Rodrigues, F. Weber, G.A. Contrera, Phys. Rev. C **89**, 015806 (2014)
17. G.A. Contrera, D. Gómez Dumm, N.N. Scoccola, Phys. Lett. B **661**, 113 (2008)
18. G.A. Contrera, D. Gómez Dumm, N.N. Scoccola, Phys. Rev. C **81**, 054005 (2010)
19. A. Scarpettini, D. Gómez Dumm, N.N. Scoccola, Phys. Rev. C **69**, 114018 (2004)
20. I.F. Ranea-Sandoval, S. Han, M.G. Orsaria, G.A. Contrera, F. Weber, M.G. Alford, Phys. Rev. C **93**, 045812 (2016)
21. M.B. Parappilly, P.O. Bownman, U.M. Heller, D.B. Leinweber, A.G. Williams, J.B. Zhang, Phys. Rev. C **73**, 054504 (2006)
22. L.F. Palhares, E.S. Fraga, Phys. Rev. C **82**, 125018 (2010)
23. M.B. Pinto, V. Koch, J. Randrup, Phys. Rev. C **86**, 025203 (2012)
24. B.W. Mintz, R. Stiele, R.O. Ramos, J. Schaffner-Bielich, Phys. Rev. C **87**, 036004 (2013)
25. G. Lugones, A.G. Grunfeld, M. Al Ajmi, Phys. Rev. C **88**, 045803 (2013)
26. D.N. Voskresensky, M. Yasuhira, T. Tatsumi, Nucl. Phys. A **723**, 291 (2003)
27. N. Yasutake, R. Lastowiecki, S. Benic, D. Blaschke, T. Maruyama, T. Tatsumi, Phys. Rev. C **89**, 065803 (2014)

28. N.K. Glendenning, Phys. Rep. **342**, 393 (2001)
29. X. Na, R. Xu, F. Weber, R. Negreiros, Phys. Rev. C **86**, 123016 (2012)
30. W.M. Spinella, F. Weber, G.A. Contrera, M.G. Orsaria, Eur. Phys. J. A **52**, 61 (2016)
31. J.D. Walecka, Ann. Phys. (NY) **83**, 491 (1974)
32. B.D. Serot, J.D. Walecka, Adv. Nucl. Phys. **16**, 1 (1986)
33. J. Boguta, A.R. Bodmer, Nucl. Phys. A **292**, 413 (1977)
34. J. Boguta, J. Rafelski, Phys. Lett. **71B**, 22 (1977)
35. J. Boguta, H. Stöcker, Phys. Lett. **120B**, 289 (1983)
36. R.D. Mellinger, F. Weber, W. Spinella, G.A. Contrera, M.G. Orsaria, Universe **3**, 5 (2017)
37. N.K. Glendenning, S.A. Moszkowski, Phys. Rev. Lett. **67**, 2414 (1991)
38. S. Typel, G. Ropke, T. Klahn, D. Blaschke, H.H. Wolter, Phys. Rev. C **81**, 015803 (2010)
39. G.A. Lalazissis, T. Niksic, D. Vretenar, P. Ring, Phys. Rev. C **71**, 024312 (2005)
40. T.A. Rijken, M.M. Nagels, Y. Yamamoto, Prog. Theor. Phys. Suppl. **185**, 14 (2010)